



HAL
open science

Comparative study of the tribological behaviour of emulsions and demoulding oils at the concrete/formwork interface

Laurent Libessart, Chafika C. Djelal Djelal, Pascale de Caro, Issam Laiymani

► **To cite this version:**

Laurent Libessart, Chafika C. Djelal Djelal, Pascale de Caro, Issam Laiymani. Comparative study of the tribological behaviour of emulsions and demoulding oils at the concrete/formwork interface. *Construction and Building Materials*, 2020, 239, <10.1016/j.conbuildmat.2019.117826>. <hal-02555850>

HAL Id: hal-02555850

<https://hal.inrae.fr/hal-02555850v1>

Submitted on 8 Jul 2022

HAL is a multi-disciplinary open access archive for the deposit and dissemination of scientific research documents, whether they are published or not. The documents may come from teaching and research institutions in France or abroad, or from public or private research centers.

L'archive ouverte pluridisciplinaire **HAL**, est destinée au dépôt et à la diffusion de documents scientifiques de niveau recherche, publiés ou non, émanant des établissements d'enseignement et de recherche français ou étrangers, des laboratoires publics ou privés.



Distributed under a Creative Commons CC BY-NC-ND 4.0 - Attribution - Non-commercial use - No Derivative Works - International License

Comparative study of the tribological behaviour of emulsions and demoulding oils at the concrete/formwork interface

Libessart Laurent^a, Djelal Chafika^a, de Caro Pascale^b, Laiymani Issam^a

^a Univ. Artois, EA 4515, Laboratoire de Génie Civil et géo-Environnement (LGCgE), F-62400 Béthune, France

^b Univ. Toulouse, Laboratoire de Chimie Agro-industrielle, LCA, , INRA, F-31030 Toulouse, France

Corresponding author: laurent.libessart@univ-artois.fr

ABSTRACT. To ensure a performing demoulding, a release agent must resist the friction of concrete on the formwork. Emulsions are interesting alternatives that leads to a reduced consumption of oil on construction sites. The behaviours of two commercial emulsions are compared with two conventional demoulding oils. The adhesion energy calculated were favourable to the emulsions. The water evaporation kinetics leads to the measurements of film thickness. Tests with the tribometer have shown that the films produced from the emulsions generate a friction reduction of 30% and 40% at the concrete / formwork interface. Such performance can be explained by Wenzel's state of wettability, which facilitates the film fit into the formwork roughness.

KEYWORDS: tribometer, friction, emulsion, adhesion energy, interface, demoulding oil

Highlights:

Adhesion energies are higher for films generated from emulsions

Films from emulsions have specificities in term of thickness and uniformity.

The vegetable-based films generate a reduction of friction on concrete.

Tribological tests confirms a Wenzel state for emulsions on the formwork

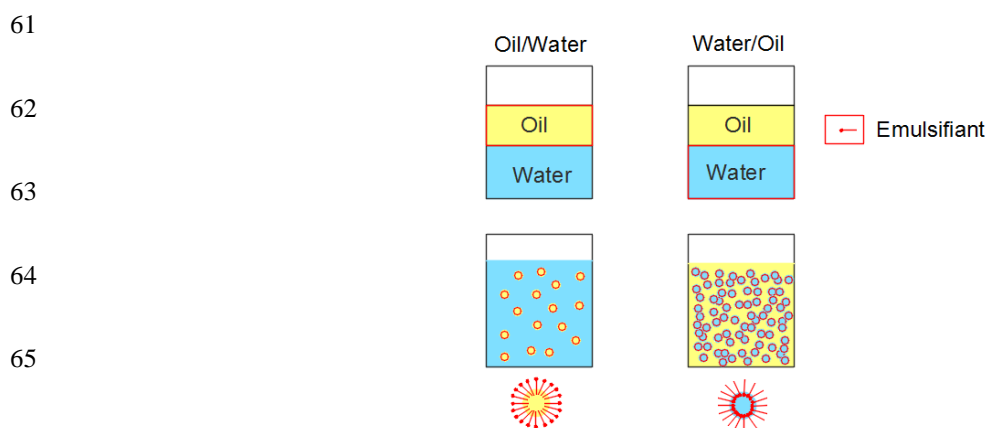
29 **1. Introduction**

30 In the building industry, concrete formwork removal has always been a complex part of construction
31 operations. Current regulations limit the use of formwork release oils to two hours per day and per user,
32 which represents severe constraints for the on-site organisation. Users attempt to make this step easier
33 by implementing new techniques, namely: the polarisation [1], the creation of self-lubricating surface
34 coatings [2], or even the application of a controlled permeable formwork liner at the interface [3]. The
35 adhesion of concrete on the formwork remains an open subject. Permeable coatings still need to develop
36 their re-use to become competitive. The mechanical characteristics of waterproof polymer coatings limit
37 their use. The use of release agents remains the most used process despite its repeatability and costs, as
38 evidenced by the number of published works [4]. Due to environmental and health impacts, the market
39 for vegetable-based products has significantly grown. In order to classify these products, the SYNAD
40 (National Union of Admixtures for Concrete and Mortar) built an abacus [5] based on the product
41 composition and the use-related criteria (safety, health, environment). While the compositions of
42 vegetable-based formulations contribute to an effective concrete setting in the formwork, defects
43 (variation in hues, micro-bubbling) can nonetheless appear in the event of an overconcentration [6,7].
44 Emulsions contains about 70 % of water, which makes it possible to apply a reduced amount of oil on
45 the formwork surface. Previous works [4,16] have already studied the configuration of films composed
46 of mineral and vegetable oils at the surface of a metal formwork, in connection with their mode of action.
47 In contrast, the behaviour of emulsions has not received much attention in the civil engineering field
48 [8]. Therefore, it seems interesting to investigate the characteristics of the film after the water
49 evaporation. To identify the specificities of the resulting film, comparisons are done between four
50 commercial demoulding agents: two emulsions and two conventional oils. The resistance of the film to
51 the moving concrete was determined by a plane/plane tribometer that represents concrete casting
52 conditions in a formwork.

53 **2. Emulsions characterization**

54 An emulsion is the dispersion of a liquid in small droplets into another immiscible liquid [9]. Thus, for
55 an oil-in-water emulsion, the oil is the dispersed phase in the water, the continuous phase. The oil

56 dispersion requires a mechanical action (homogeniser) in order to form minuscule droplets [10]. The
 57 addition of an emulsifier that lowers the interfacial tension between the two phases, improves the
 58 physical stability of the mixture by forming micelle [8] (Fig. 1). Creaming or sedimentation refers to a
 59 process leading to a phase separation. Emulsions are widely used in the cosmetics, food processing,
 60 paint and construction industries.



67 **Fig. 1.** Diagram of the direct emulsion O/W and invert W/O

68 Table 1 lists the characteristics of the four demoulding oils supplied by a manufacturer. An invert
 69 mineral emulsion (IME) and direct vegetable emulsion (DVE) are compared to a vegetable oil-based
 70 product (V) and a mineral oil-based product (M).

71 **Table 1** Properties of release agents

	DVE	IME	V	M
Type	Direct emulsion	Invert emulsion	Oil	Oil
Composition	Vegetable esters	Paraffinic wax	Vegetable esters	Paraffinic hydrocarbons
Oily phase	Vegetable	Mineral	Vegetable	Mineral
Content of water (%)	80	70	0	0
Flash point °C	> 100	96	>100	>100
Viscosity (mPa.s)	38.5±1.5	60.6±3.4	66.6±2.8	24.5±1.7
Density	< 1	< 1	0.93	0.86

72

73 The dynamic viscosity is determined using a HAAKE VT550 single-speed viscometer, fitted with a 1°
 74 (PK5) cone. A constant volume of oil ($v = 0.6 \text{ cm}^3$) is deposited on the plate, and the cone is lowered

75 toward the plate. As expected, the direct emulsion has a lower viscosity than for invert emulsion, due to
 76 a lower content in oil. The contents of water were given by the supplier.

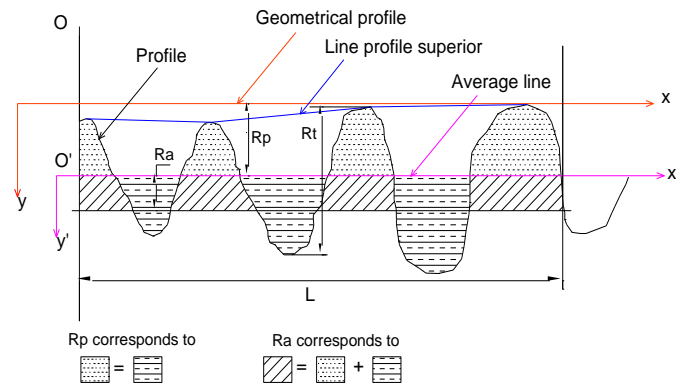
77 2.1. Surface state of formwork

78 Metal formwork is extensively present in the building trades; it serves to streamline concrete setting and
 79 enhance worksite productivity. The potential for formwork reuse is substantial for these structural
 80 elements repeated throughout a project, i.e. vertical shear walls, floors and columns. A new steel
 81 formwork was chosen, and its surface roughness was measured. Samples were cut from the formwork
 82 surface to perform microscopy tests and to measure film thicknesses. The parameters (Fig. 2) chosen to
 83 evaluate roughness are as follows [11]:

84 Ra: arithmetic mean of profile deviations relative to the average line.

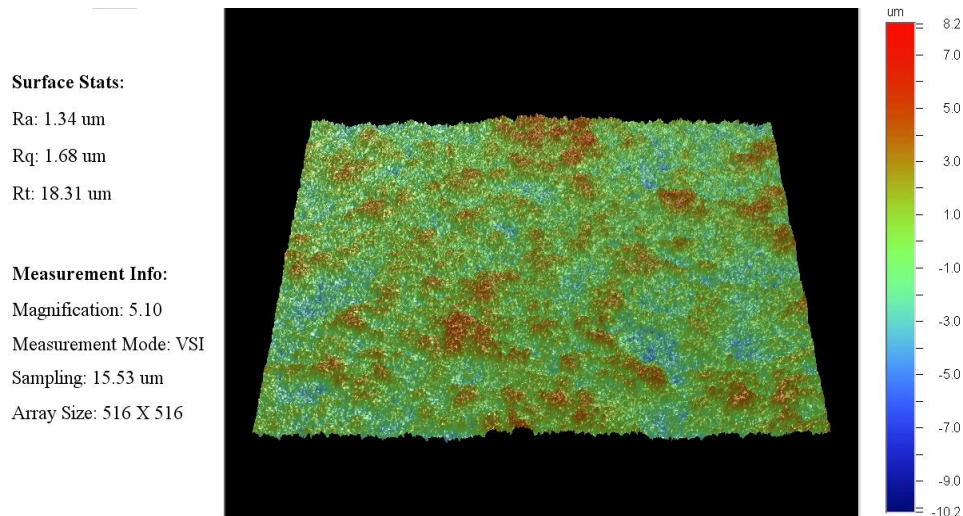
85 Rp: average depth over an evaluation length.

86 Rt: peak height at the maximum profile valley.



89 **Fig. 2.** Scheme of the roughness profile (height vs. length).

90 Figure 3 displays a 3D view of the roughness profile of the formwork sample using a white-light
 91 interferometry microscope (WLIM) VEECO NT3300 over a $4 \times 4 \text{ mm}^2$ area [2]. The surface was sampled
 92 at 2052×2052 points with a $1.9 \mu\text{m}$ step scale along X- and Y-directions. For this sample, an average
 93 roughness value Ra of $1.34 \mu\text{m}$, a maximum Rt profile deviation of $18.31 \mu\text{m}$, a Rp value of $3.28 \mu\text{m}$,
 94 and a value dispersion on the image of ± 0.02 . The profile values between 8 and $-10 \mu\text{m}$ and the low
 deviation, indicated that the formwork surface has a low roughness, uniform on the sample.



95

96

Fig. 3. 3D image of the new formwork roughness profile

97 Further measurements have been made on a roughness meter [11] on ten measuring points to obtain a
98 more precise representation of the formwork roughness. The average values are given in Table 2. The
99 dispersion value is $\pm 0.02 \mu\text{m}$.

100 **Table 2.** Roughness parameters of the formwork sample.

Test	1	2	3	4	5	6	7	8	9	10	Average
Ra (μm)	1.32	1.23	1.35	1.13	1.41	1.18	1.18	1.38	1.26	1.15	1.26
Rt (μm)	13.53	13.23	15.54	12.53	15.67	13.87	13.65	18.56	16.98	13.23	14.68
Rp (μm)	2.69	3.17	3.76	3.08	4.05	3.45	2.98	3.65	4.12	3.07	3.40

101

102 Roughness values obtained by the two methods are in agreement with those of a new formwork surface
103 used on site. [6].

104 2.2. Interfacial properties

105 The assessment of release agent performances implies the characterization of the interface in contact
106 with the support. The affinity of oil with the support is a significant property since the oil film acts as a
107 protective coating for the formwork and plays the role of a lubricant during the concrete casting step
108 [6].

109 As a matter of fact, the liquid/vapor surface tension of a liquid is correlated with the value of the contact
110 angle formed by a drop on a support [12]. Contact angles are a readily observed physical phenomenon
111 related to the more fundamental concepts of energy and surface tension. This insight helps determine

112 the properties of wettability and adhesion of a film, which in turn makes it possible to predict the
 113 properties of a coating or detect traces of surface pollutants. As part of a theoretical approach, adhesion
 114 energy values are calculated based on contact angle data. It may be considered that the liquid/solid
 115 adhesion energy value is representative of the adhesive strength between the liquid and the support.

116 The liquid/solid adhesion energy value also represents the adhesive force between a liquid and a support.

117 Adhesion energies are calculated according to Zisman's Equation [13]:

$$118 \quad \omega_{LS} = \gamma_{LV} \times (1 + \cos \theta) \quad (1)$$

119 The liquid/vapor surface (γ_{LV}) tension was measured using Wilhelmy's plate method at 20°C. The device
 120 employed is a tension meter manufactured by the CAD firm and fitted with a platinum blade. The surface
 121 tension is indicated by the meniscus formed along the plate boundary. The material contact angle (θ) was
 122 then determined by a PGX type of mobile goniometer. This device measures the contact angle at the
 123 interface between a liquid drop and the substrate surface where the drop has been deposited [14].

124 Table 3 summarises adhesion energy values at 20°C. We can observe that emulsions have higher
 125 adhesion energies than oils, which is a necessary condition to reduce frictions. Higher adhesion energy
 126 corresponds to higher surface tension and lower drop angle.

127 **Table 3.** Interfacial properties of release agents at 20 °C

	Surface tension L/V (mN/m)	Contact angle (°)	Adhesion energy L/S (mN/m)
DVE	40.0	33.1	73.50
IME	37.1	22.5	71.35
V	33.4	32.8	61.5
M	30.6	18.5	59.6

128

129 **2.3. Formation of the oil film**

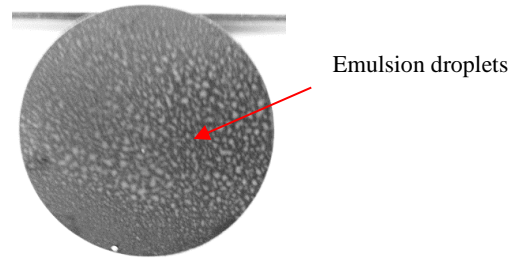
130 Demoulding oils were applied in a regular manner at a distance of 15cm from the surface of a formwork
 131 sample (disk with a diameter of 5 cm) using an Ecospray sprayer fitted with a conical nozzle of 1 mm
 132 diameter (Fig. 4).

133

134

135

136



137

Fig. 4. Surface state after spraying on the formwork

138

139

140

141

142

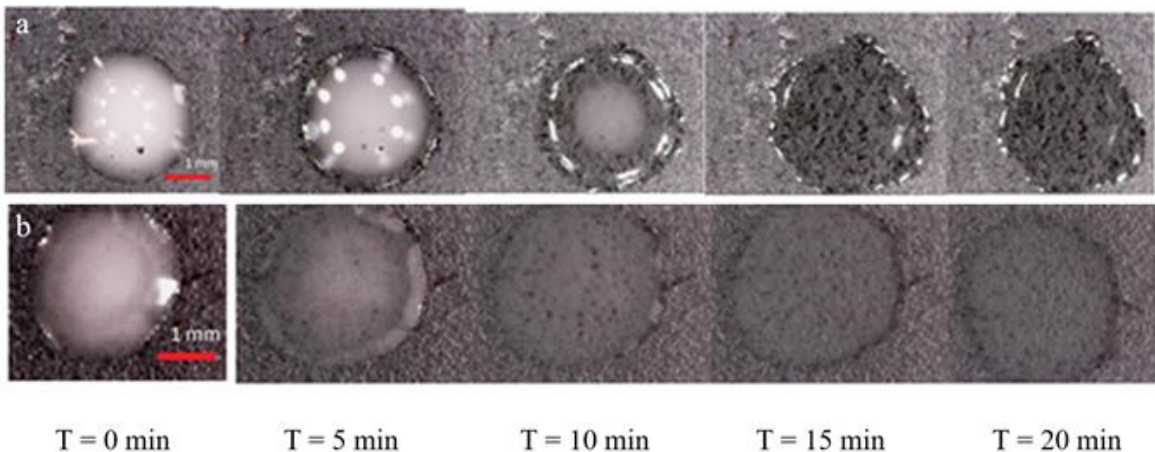
143

144

145

146

A cloud of white droplets fell on the surface. Then, a latency period occurs during the evaporation of water. The time elapsed has been estimated by the supplier at 15-20 min. During this latency period, the emulsion film formation was in progress and was analysed by means of optical microscopy (Figs. 5 and 6). As the water gradually evaporated, the emulsified medium became structured. On the emulsion micrographs, the white colour denotes the emulsified phase, which tends to disappear in favour of the oily phase. The observations conducted under optical microscopy of a single drop showed that, for the invert emulsion, water disappeared more quickly compared to direct emulsion water (white colour no longer visible). Similarly, the reverse emulsion drop diameter increased rapidly (+20% after 5 min), which indicates that the film began to form at the surface.



147

148

149

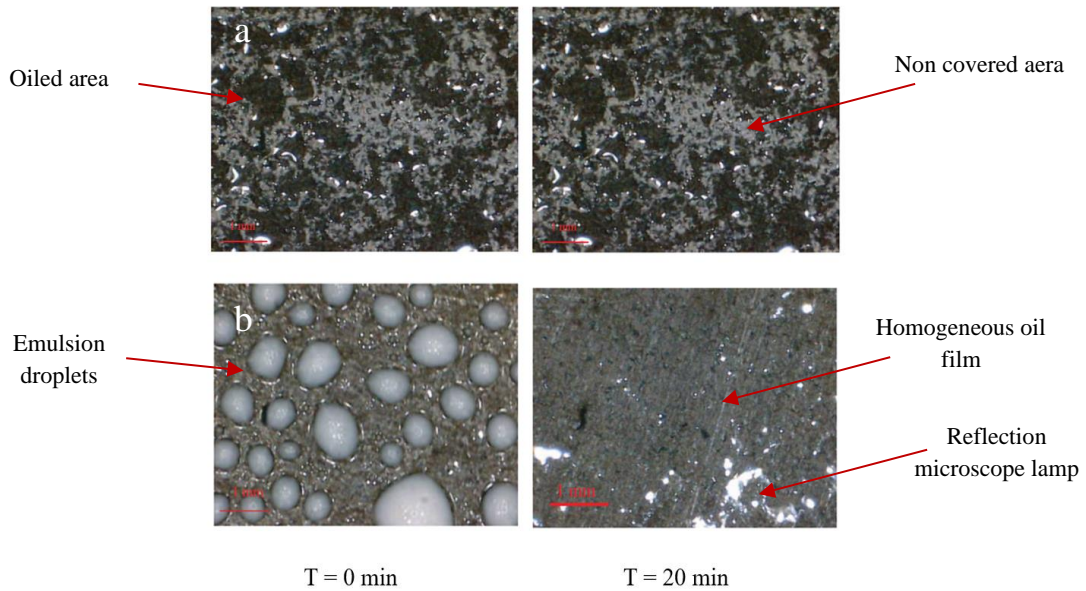
150

151

Fig.5. Evolution of a drop of (a) DVE and (b) IME emulsions during the latency period

Micrographs were taken 20 min after spraying of DVE emulsion and vegetable oil (V) on two formwork samples. After the oil droplets has merged, DVE emulsion has generated a film with a uniform distribution over the formwork surface (Fig. 6). We can observe that the vegetable oil film has a lesser

152 coating rate. In fact, previous works have shown that it was necessary to scrape the vegetable oil film to
 153 improve its homogeneity [15].



154

155 **Fig. 6.** Film micrographs after spraying (a) the V oil and (b) the DVE emulsion

156 During the latency period, a monitoring of the emulsion deposited onto the new formwork samples was
 157 carried out

158 The thickness of film (e) depends on the mass (m) of product on the plate, its density (ρ) and the plate
 159 surface (S). Weighing was performed with a precision scale of 10^{-4} g [6].

$$160 \quad V = S \times e \Leftrightarrow e = \frac{V}{S}; \quad V = \frac{m}{\rho}; \quad \text{then} \quad e = \frac{m}{\rho \times S} \quad (2)$$

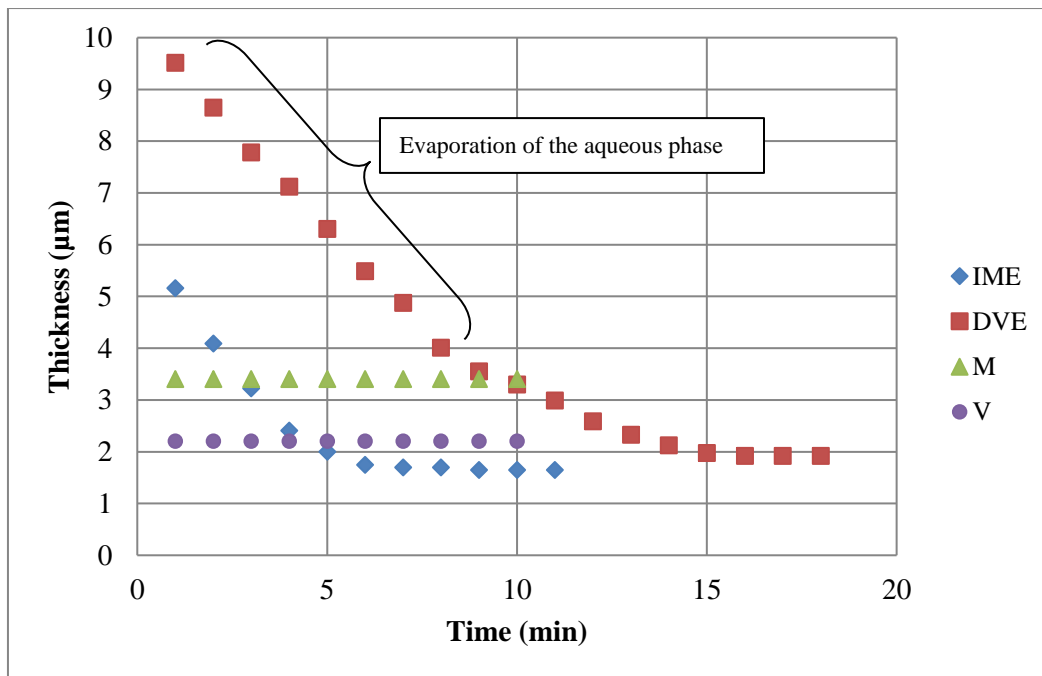
161 with S (m^2), ρ (kg/m^3), m (kg), and e the thickness (m).

162 Previous works have shown that values obtained by the weighing method were very close to
 163 measurements carried out by PIXE [16]. It was found that the film thicknesses for conventional oils are
 164 typically between 3 and 4 μm for a mineral oil and between 2 and 3 μm for a vegetable oil [4].

165 A monitoring of film thickness variation over time was carried out. (Fig. 7). The reproducibility of
 166 measurement is based on four tests.

167 One test was conducted by spraying 0.0168 g of DVE and 0.0101 g of IME on two formwork samples.

168 The lower viscosity of DVE led to deposit a slightly higher mass of DVE.



169
170 **Fig. 7.** Water evaporation kinetics for the deposited emulsions

171 The final thickness of the oil film after complete water evaporation was determined by weighing. The
172 aqueous phase is completely evaporated when the film mass remained constant, which corresponds to
173 the final oil film thickness. Seven minutes were required for the film formation with the invert emulsion
174 and 16 minutes with the direct emulsion, which is in agreement with their water content (table 1). Thus,
175 the direct emulsion lost 79% of its initial mass, whereas the decrease of mass was close to 67% for the
176 invert emulsion. The direct emulsion film reached an average thickness of $1.9 \pm 0.2 \mu\text{m}$, while the invert
177 emulsion film was $1.7 \pm 0.2 \mu\text{m}$ thick (averaged over 4 tests). The difference between the two initial
178 masses was 39.9%, but the final film thicknesses were very close, because of the higher evaporation rate
179 of the direct emulsion. For the mineral emulsion, the reduction in thickness was 47% compared to the
180 mineral oil, whereas the reduction was 14% for vegetable emulsion compared to the conventional
181 vegetable oil. Indeed, the active fractions in VDE is lower compared to that of IME. Finally, in both
182 cases, emulsions generated thin oil films with high adhesion energies, especially for the mineral oil.

183 3. The friction of the concrete on the formwork

184 An experimental campaign has been conducted in order to assess the resistance of these films to concrete
185 friction using a plane/plane tribometer. Previous studies [4,15] have shown that this level of resistance
186 is connected to the aesthetic quality of concrete facing and depends on the mechanisms at the interface

187 and on the type of oil. The performances of a mineral film are driven by its thickness. A vegetable-based
 188 film contains fatty acids contributing to an interfacial organization in layers.

189 3.1. The concrete

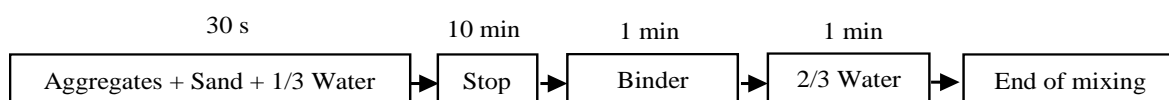
190 The concrete used is a traditional mix with a water-to-binder (W/B) ratio of 0.57 and a gravel-to-sand
 191 (G/S) ratio equal to 1.27. The workability measured with the Abrams cone, is between 12 and 14 cm,
 192 which corresponds to the S3 consistency class (according to Standard NF EN 206-1). The relevant mix
 193 design is given in Table 4.

194 **Table 4.** Concrete formulation

Concrete	(kg/m ³)
Cement CEM I 52,5 CP2	265
Fillers	88
Sand 0/4	792
Gravel 4/8	271
Gravel 6/20	734
Water	201

195

196 The concrete production requires a well-defined mixing protocol. Standard NF P 18-404, entitled
 197 "Concretes - Design, suitability and inspection testing - Specimen production and conservation", was
 198 implemented. The mixing procedure was performed with dry materials according to this protocol:



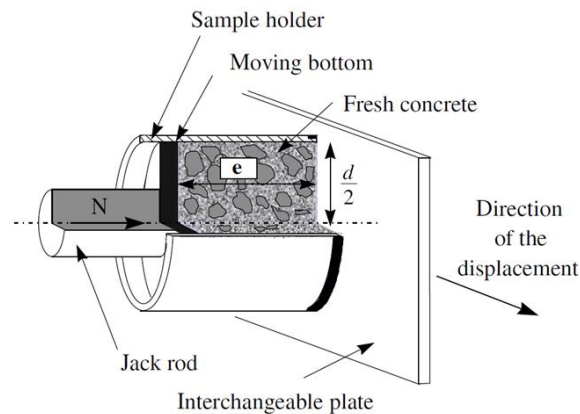
199

200 Tests were carried out at a temperature of 20°C.

201 3.2. The plane/plane tribometer

202 A plane/plane tribometer was developed by our team and was patented under the number PCT/EP
 203 2017068017. The principle behind this test set-up (Fig. 8) is as follows [4]: an interchangeable plate
 204 slides between two fresh concrete samples, with the movement being carried out using a motor coupled
 205 to an auger. The plate speed is controlled by a programmable controller. The samples are pressurised by

206 means of jacks, with the pressure lying between 50 kPa and 500 kPa. A force sensor connected to the
 207 plate measures the tangential stresses acting on the plate due to the concrete.



208

209

Fig 8. Concrete tribometer principle [4]

210

3.2.1. Experimental conditions

211

For the experimental campaign, the test parameters replicated worksite conditions in order to approximate the stresses being exerted on the oil film by the concrete. The casting speed and pressures at the formwork base constitute the key parameters of the study. Tests were conducted on a plate cut-out from a formwork wall with roughness values of $R_a = 1.34 \mu\text{m}$. The emulsions were applied by spraying in full compliance with the supplier recommendations.

214

216

3.2.2. Casting speed

217

The plate displacement speed corresponds to the casting speed of a concrete shell extending over a certain height. For our testing campaign, a speed of 3 m/h (0.84 mm/s) was used, which corresponds to the speed most commonly practiced on worksites [18].

219

220

3.2.3. Contact pressure

221

The contact pressure of the selected jack corresponds to the concrete pressures being exerted at the formwork base for a given height. The vertical formwork elements are subjected, as a result of the fresh concrete, to a thrust perpendicular to the shuttering surface. The factors capable of influencing this

223

224 pressure exerted on the formwork consist of: specific gravity of the concrete, workability measured
 225 using Abrams' cone, height of fresh concrete, minimum formwork dimension, and filling speed.

226 Considering fresh concrete as a fluid, the distribution of the pressure is triangular. The hydrostatic thrust
 227 (P) is given in Pascal by the following formula:

$$228 \quad P = \gamma \times h \quad (3)$$

229 with γ the concrete density estimated at 25 kN/m^3 and h the height of the formwork (m)

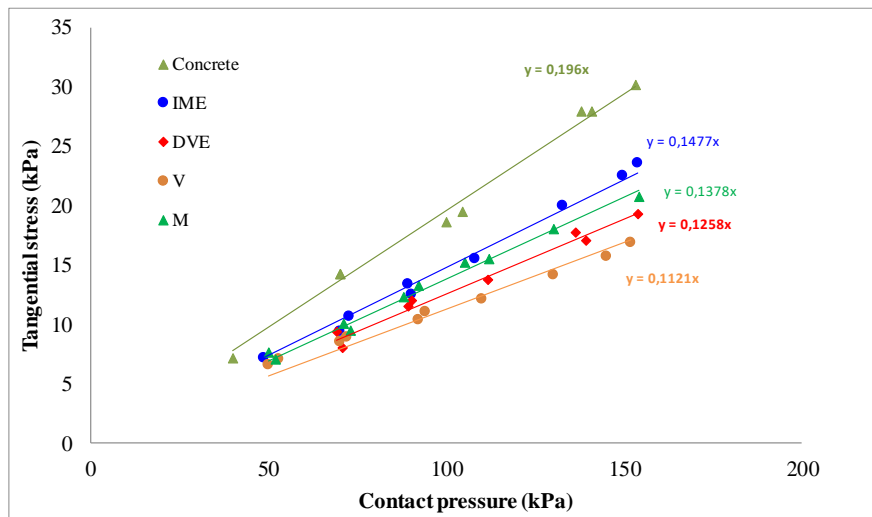
230 Shell heights ranging from 2 to 6 m have been evaluated; they correspond to pressures in the range of
 231 50 to 150 kPa.

232 4. Analysis of the formwork/concrete interface

233 Friction stresses vs. contact pressure for the fresh concrete and for formwork release agents are shown
 234 in Figure 9. A Coulomb law is applied in this pressure range:

$$235 \quad \tau_f = \mu \times P \quad (4)$$

236 with τ_f the tangential stress (Pa) and P the contact pressure (Pa).



237
 238 **Fig 9.** Dynamic friction constraints according to the pressure ($v = 0.84 \text{ mm / s}$)

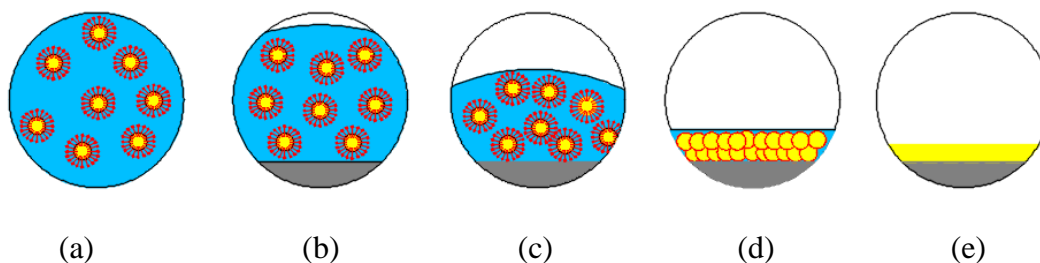
239
 240 The stress variations vs. contact pressure indicate an average decrease in friction stresses of 30% for
 241 IME and up to 40% for VDE, compared to the interface without any demoulding agent. The oil films
 242 from emulsions thus contribute to a significant reduction in concrete friction against the formwork, even

243 despite thin films (between 1.5 and 2 μm). We can note that the vegetable-based films (oil or emulsion)
 244 prove to be more efficient in contact with concrete, compared to the both mineral films.

245 A previous study of the oil/concrete interface has described two behaviours: a lubricating effect
 246 mainly due to a physical action for mineral oils and a chemical action of the vegetable-based
 247 formulations [15]. Thanks to triglycerides, fatty acids and other esters as ingredients in a vegetable
 248 formulation, carboxylates (soap) are formed in contact with concrete (basic medium), which can explain
 249 the lower frictions observed.

250 5. Discussion

251 This study describes the film formation generated from an emulsion and its main characteristics. Before
 252 spraying, protected from the air, the direct emulsion (DVE) is stable (Fig. 10), and the oily micelles are
 253 dispersed in the emulsion (Fig. 10a). After spraying, a set of droplets forms on the formwork surface;
 254 water is still present in a large quantity, and the micelles are still mobile (Fig. 10b). As the water
 255 gradually evaporates, the film becomes reconfigured and the micelles are directed towards the formwork
 256 surface. Due to their chemical adsorption, the film can adhere to the surface (Fig. 10c). In conclusion,
 257 the polarity of the metal surface makes it possible to correctly direct the micelles (Fig. 10d); meanwhile,
 258 the droplets combine to form a homogeneous oil film on the surface (Fig. 10e) [17]. In the case of the
 259 invert emulsion (IME) (Fig. 11), the aqueous phase is composed of smaller-sized and more numerous
 260 water micelles compared to the direct emulsion (Fig. 11a). Over time, the water micelles occupy less
 261 volume (Figs. 11b, 11c). This process forces the oily phase to move towards the formwork (Fig. 11d).
 262 Ultimately, the water contained in the micelles evaporates and the film becomes homogeneous (Fig.
 263 11e).



264

265

266

Fig. 10. Evolution diagram of the direct emulsion over time

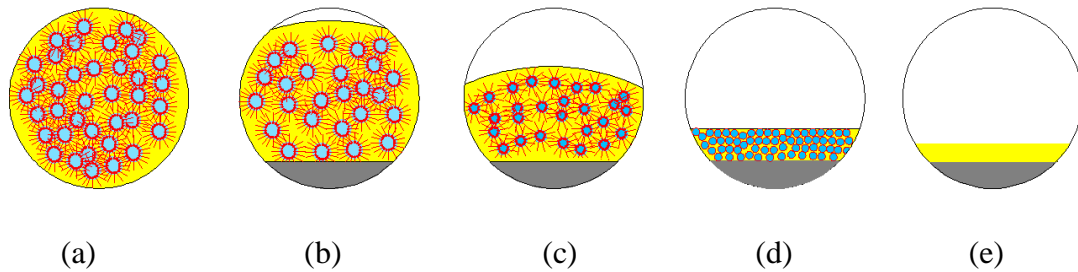
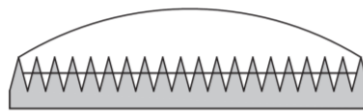


Fig. 11. Evolution diagram of the invert emulsion over time

267
268
269
270
271
272
273
274
275

To understand the phenomena at the emulsion/formwork interface, it is necessary to focus on the roughness of the plate. In fact, a sprayed oil tends to remain at the surface of the formwork asperities [11]. In contrast, the micelles (whether direct or invert) in emulsion have a size (0.02 and 0.2 μm) facilitating their insertion into the plate surface roughness (Fig. 2). In this case, the Wenzel wettability state [19] has been reached, as opposed to the conventional oils, which are in a Cassie state [20] (Figure 12).



276
277

Fig. 12. Schematic representation of the Cassie state for conventional oil on a new formwork [11]

278
279
280
281
282
283
284
285

The measured surface tensions are greater than the conventional oils, this validates the Wenzel state for emulsions. According to Wenzel state, the film obtained after evaporation of the aqueous phase is totally inserted into the roughness of the plate, thus generating a homogeneous film, covering the whole surface. According to the work of Bormashenko [21, 22], figure 13 illustrates the Wenzel state for an emulsion. The film of IME is anchored more quickly in the formwork asperities in fact, the micelles of water evaporate faster. In both cases, despite a lower weight, the consequence of this configuration is the formation of an oily film, more resistant to the contact with the concrete.

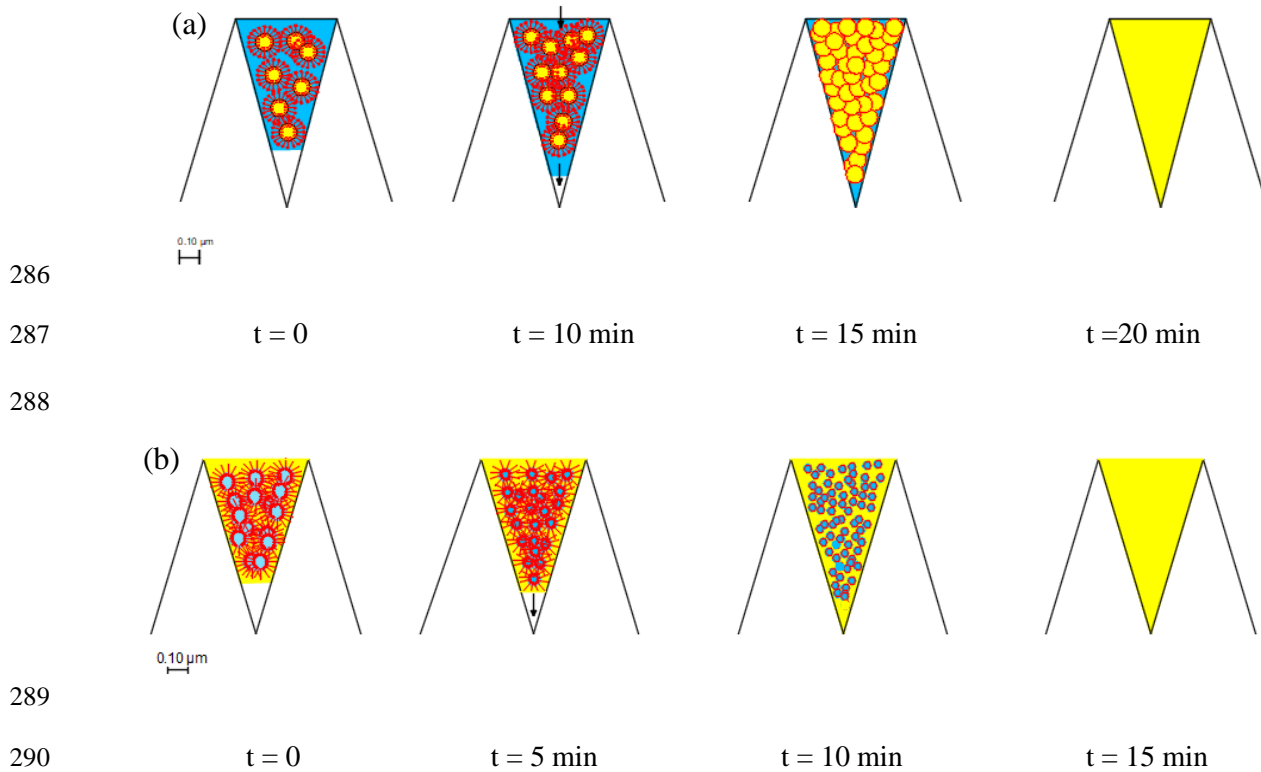


Fig. 13. Schematic evolution of (a) DVE and (b) IME emulsion films towards Wenzel state [21]

6. Conclusion

Emulsions exhibit a set of specific physicochemical properties. Their spraying on a formwork surface is followed by a water evaporation phase, along with the oily phase organization, leading to the formation of a rather thin oil film. The water evaporation profile indicated that the latency period may vary from 6 to 15 min, which is in agreement with the time period mentioned by the manufacturers. The film micrographs (20 min after spraying the emulsion) showed that the film formed as the oil droplets merge displayed a homogeneous distribution of oil on the formwork. Furthermore, the emulsions demonstrated a tribological behaviour similar to that of the conventional oils, i.e. resulting in a significant stress reduction. The formation of the lipophilic film as the aqueous phase evaporated is most likely related to micelle migration into the formwork roughness. This process helps improve the lubricating effect between concrete and formwork, as the oil film is reconfigured by interacting with the formwork roughness and do not need to be scrapped. The use of emulsions as a formwork release agent represents an efficient alternative to combine technical performance with a lower content of active ingredients. Vegetable formulations remain more effective compared to mineral formulations. They

306 should continue to develop on worksites over the near term. Other tests could bring further data about
307 the appearance of concrete facings demoulded with emulsions, or by involving other techniques (CPF
308 film, wood formwork, ...).

309

310 **References**

311 [1] Goudjil N, Djelal C, Vanhove Y, Kada H, Heloun N. Impact of temperature on the demoulding of
312 concrete elements with a polarization process. *Constr Build Mater* 2014;54:402-412.

313 [2] Spitz N, Coniglio N, El Mansori M, Montagne A, Mezghani S. On functional signatures of bare and
314 coated formwork skin surfaces. *Constr Build Mater* 2018;189:560–567.

315 [3] Kothandaraman S, Kandasamy S. The effect of controlled permeable formwork (CPF) liner on the
316 surface quality of concretes. *Cem Conc Comp* 2017;76:48-56.

317 [4] Djelal C, De Caro P, Libessart L, Dubois I. Comprehension of demoulding mechanisms at the
318 formwork/oil/concrete interface. *Mater Struct* 2008;41:571–81.

319 [5] Syndicat national des adjuvants pour bétons et mortiers (SYNAD) (2014) Classification Synad des
320 agents de démoulage.

321 [6] Libessart L, Djelal C, De Caro P. Influence of the type of release oil on steel formwork corrosion
322 and facing aesthetics. *Constr Build Mater* 2014;68:391–401.

323 [7] Liu, Yang, Xie. Factors influencing bugholes on concrete surface analyzed by image processing
324 technology. *Constr Build Mater* 2017;153:897–907.

325 [8] Leon-Martinez FM, Abad-Zarate EF, Lagunez-Rivera L, Cano-Barrita PF de J. Laboratory and field
326 performance of biodegradable release agents for hydraulic concrete. *Mater Struct* 2016;49: 2731–2748.

327 [9] Ushikubo FY, Cunha RL. Stability mechanisms of liquid water-in-oil emulsions. *Food Hydro*
328 2014;34:145-153.

329 [10] Fingas M, Fieldhouse B. Studies of the formation process of water-in-oil emulsions. *Mar Pol Bul*
330 2013;47:369–396.

- 331 [11] Libessart L, de Caro P, Djelal C, Dubois I. Correlation between adhesion energy of release agents
332 on the formwork and demoulding performances. *Constr Build Mater* 2015;76:130-139.
- 333 [12] Chappuis, J.; Georges, J-M. Contribution to Study of Wetting - Analysis of a Measuring Method.
334 *J Chim Phys Phys Chim Biol* 1974;71:567-575.
- 335 [13] Zisman WA. Relation of the equilibrium contact angle to liquid and solid constitution. *Advances*
336 *in chemistry*. American Chemical Society; 1964. p. 1–51.
- 337 [14] Libessart L, Djelal C, De Caro P, Vanhove Y (2014) Influence de l'énergie d'adhésion des huiles
338 de démoulage sur le frottement du béton. 26ème Journées Internationales Francophones de Tribologie,
339 Mulhouse, France, Presse des Mines, pp189-197.
- 340 [15] de Caro P, Djelal C, Libessart L, Dubois I. Influence of the nature of the demoulding agent on the
341 properties of the formwork–concrete interface. *Mag Concr Res* 2007;59:141–9.
- 342 [16] Djelal C, Vanhove Y, Chambellan D, Brisset P. Influence of the thickness of demoulding oils on
343 the aesthetic quality of facings. *Mater Struct* 2010;43:687-698.
- 344 [17] Gutiérrez G, Benito JM, Coca J, Pazos. Evaporation of aqueous dispersed systems and concentrated
345 emulsions formulated with non-ionic surfactants. *Inter Jour Heat Mass Trans* 2014; 69:117-128.
- 346 [18] Gardener NJ. Pressure of concrete on formwork, *ACI J*. 1985, pp744 – 753.
- 347 [19] Lafuma A, Quéré D. Superhydrophobic states. *Nat Mater* 2003;2:457-460.
- 348 [20] Lee J, Hwang S-H, Yoon S-S, Khang D-Y. Evaporation characteristics of water droplets in Cassie,
349 Wenzel, and mixed states on super hydrophobic pillared Si surface. *Col Surf A: Physand Eng Asp*,
350 2019;562:304-309.
- 351 [21] Bormashenko E. Progress in understanding wetting transitions on rough surfaces. *Adv Colloid*
352 *Interf Sci* 2015 ;222:92-105.
- 353 [22] Bormashenko E. Apparent contact angles for reactive wetting of smooth, rough, and heterogeneous
354 surfaces calculated from the variational principles. *Jour Col Interf Sci* 2019 537 :597–603